Front. Earth Sci. 2021, 15(3): 507–525
https://doi.org/10.1007/s11707-021-0904-y

RESEARCH ARTICLE

Urban spatial structure analysis: quantitative identification of urban social functions using building footprints

Zhiyao ZHAO[1], Xianwei ZHENG (✉)[2], Hongchao FAN[3], Mengqi SUN[1]

1 School of Remote Sensing and Information Engineering, Wuhan University, Wuhan 430072, China
2 State Key Laboratory of Information Engineering in Surveying, Mapping and Remote Sensing, Wuhan University, Wuhan 430072, China
3 Department of Civil and Environmental Engineering, Norwegian University of Science and Technology, Trondheim 7491, Norway

Abstract Analysis of urban spatial structures is an effective way to explain and solve increasingly serious urban problems. However, many of the existing methods are limited because of data quality and availability, and usually yield inaccurate results due to the unclear description of urban social functions. In this paper, we present an investigation on urban social function based spatial structure analysis using building footprint data. An improved turning function (TF) algorithm and a self-organizing clustering method are presented to generate the variable area units (VAUs) of high-homogeneity from building footprints as the basic research units. Based on the generated VAUs, five spatial metrics are then developed for measuring the morphological characteristics and the spatial distribution patterns of buildings in an urban block. Within these spatial metrics, three models are formulated for calculating the social function likelihoods of each urban block to describe mixed social functions in an urban block, quantitatively. Consequently, the urban structures can be clearly observed by an analysis of the spatial distribution patterns, the development trends, and the hierarchy of different social functions. The results of a case study conducted for Munich validate the effectiveness of the proposed method.

Keywords urban spatial structure, variable area unit (VAU), spatial metric, social function likelihood, OpenStreetMap

1 Introduction

With the rapid development of the urban social economy and the fast expansion of urban areas in recent decades, traffic congestion (Arnott, 1998), long commuting distances (Gordon et al., 1989; Sohn, 2005), energy consumption (Le Néchet, 2012), urban sprawl (Lv et al., 2012; Ding and Zhao, 2014), urban environmental issues (Burgalassi and Luzzati, 2015), and employment imbalance (Simpson, 1992; Boarnet et al., 2017) have become serious issues. These urban problems are the outcome of the interaction of multiple factors, including economic, social, political, and cultural influences, which all affect the arrangement of the urban space and contribute to forming the urban spatial structure. The urban spatial structure, in turn, reflects the dynamic change, the spatial layout of the urban structure elements, and the underlying interactions of a city (Anas et al., 1998). The detection and analysis of the urban spatial structure are thus widely regarded to explain and solve urban issues. The capacity and efficacy of urban spatial structure analysis in the exploration and prediction of urban morphology and dynamics have been repeatedly demonstrated (Zhang, 2008; Zhong et al., 2014). Therefore, it is essential to exploit an effective urban spatial structure analysis method when attempting to solve the increasingly serious urban problems.

Researchers have strived to identify and describe the elements of urban spatial structure effectively (Zhong et al., 2013; Chen et al., 2017b) with different proxies. One of the popular ways for urban spatial structure analysis is to utilize the arrangement of the urban space with respect to the social function types. With different data as input, a great number of methods have been devoted to the identification and analysis of urban social function elements, which can be generally categorized into four groups: 1) land-cover based methods; 2) urban activity based methods; 3) urban network based methods; and 4) building layout based methods.

The land-cover based methods usually use remote sensing methods to map the land cover and thus analyze the underlying social function elements (Heiden et al., 2012). However, remote sensing methods have several

Received May 25, 2020; accepted April 20, 2021

E-mail: zhengxw@whu.edu.cn

drawbacks, as the data quality and error in the object classification can reduce the classification quality of urban functional zones (Zhang et al., 2017). Moreover, the existing frequently used machine learning or deep learning (Huang et al., 2018) techniques for land-use mapping (Zhang et al., 2019a) are highly dependent on training samples (Grippa et al., 2018). Some researchers have identified urban spatial structure by focusing on the analysis of the spatial distribution patterns of the various urban activities by using crowdsourced data, such as information and communication technology (ICT) data (Chen et al., 2017a), social media data (Chen et al., 2017a), and point of interest (POI) data (Yang et al., 2018). Nevertheless, the reliability of the analysis results cannot be guaranteed, in that the acquisition of crowdsourced POI data mainly relies on volunteers, without effective quality control. Even though the POI data from private companies can provide relatively accurate locations and attributes, the high cost is a limiting factor (Zhang et al., 2019b). As for urban network based methods, taxi GPS data (Qi et al., 2011; Pan et al., 2012) and smart card data (Zhong et al., 2014) have been employed to analyze land use. However, the position drift and noise of taxi GPS data can lead to uncertainty in the trajectory analysis (Liu et al., 2012; Long and Shen 2015). Moreover, public transportation represents only a small fraction of the entire urban transportation network, and the sample bias inherently existing in smart card data and trajectory data can lead to one-sidedness and a low-reliability result (Joh and Hwang, 2010).

Compared with the aforementioned categories of methods, the use of building layouts extracted from building footprints for urban social function element extraction and urban structure analysis cannot only guarantee high data quality and reliability, but it also comes with a lower acquisition cost (Xing and Meng, 2020). Based on building footprint data, researchers have attempted to identify urban functional zones, either at the building scale (Hermosilla et al., 2014) or the patch scale (Yoshida et al., 2005), with different spatial metrics. However, limitations can be found in the application of the existing spatial metrics (Steiniger et al., 2008), for example, the incorrect identification of urban functional zones caused by the lack of spatial metrics for describing the spatial distribution of buildings (Vanderhaegen and Canters, 2017). The building distribution pattern is a basic element for urban functional zone identification, since it reflects the interaction of many complex factors, such as the urban history, economy, topography, infrastructure, urban planning, and policy (Louw, 2011). However, there are few specialized spatial metrics for building distribution patterns, leading to inaccurate delineation of urban functional spaces with the building layout based methods (Xing and Meng, 2018). Another drawback is the uncertainty of the spatial analysis results caused by the scale effect of the used spatial metrics (Grippa et al., 2018). In addition to the spatial metric limitations, there are also deficiencies in the evaluation of urban functional zones. In the existing urban spatial structure analysis methods, each analysis unit is usually identified with a single social function. However, with rapidly developing urban areas, the social functions of an urban unit become more complex and diverse, which means that applying a single functional type to an urban unit is not accurate.

Based on the above observations, an investigation of social function based spatial structure analysis using building footprint data is presented in this paper. To alleviate the uncertainty of the spatial structure analysis resulting from the scale effect, the variable area unit (VAU) is first proposed as the basic spatial unit. The VAU is a spatial unit that is generated from building clusters with high homogeneity. VAU-based spatial metrics are then proposed to describe and measure the morphological characteristics and the spatial configuration of the clustered buildings in an urban block. According to the different morphological and geometric characteristics, as well as the layout of buildings shown by the different social function types (i.e., residential, industrial, commercial), the proposed VAU-based spatial metrics are assembled with two existing applicable spatial metrics to formulate better models for calculating the social function likelihoods of each urban block. It is worth mentioning that we do not identify a single function type for each urban block, as in the existing methods. Instead, we use the calculated social function likelihoods to quantitatively describe the mixture degree of a block with respect to the three types of social functions. By accurately describing the social function types that an urban block carries, a hot and cold spot analysis can then be performed to investigate the spatial distribution pattern and development trend of each type of social function in a city at a global scale. Furthermore, we also propose graph-based difference minimum spanning tree (DMIST) and difference maximum spanning tree (DMAST) analysis based on the calculated social function likelihoods, which exploits the hierarchical information of the spatial distribution of the social functions and the interaction between urban blocks in a city.

The rest of this paper is organized as follows. In Section 2, the urban block social function identification is described, including the generation of the VAU, the definition of the VAU-based spatial metrics, and the construction of the function likelihood models. The function likelihood based urban spatial structure analysis is also presented. The results of the case study conducted for the city of Munich are given in Section 3. The discussion and conclusion are provided in Section 4.

2 Methods

The method presented in this paper is composed of two main parts: 1) identification of urban block social function;

and 2) social function likelihood-based urban spatial structure analysis. The workflow of the proposed approach is shown in Fig. 1.

2.1 Identification of urban block social function

The identification of urban block social function consists of three steps: 1) the generation of the VAU; 2) the definition of the VAU-based spatial metrics; and 3) the calculation of the social function likelihood.

2.1.1 Generation of VAU

According to Tobler's first law of geography, buildings with adjacent spatial locations and similar architectural characteristics are likely to have similar social functions. To better cluster and describe those buildings with a similar social function, and eliminate the analysis uncertainty resulting from the scale effect, we employ the VAU as the spatial unit of analysis. The uncertainty in geographic information systems in classical spatial analysis methods are summarized (Zhang and Goodchild, 2002). Innovative concepts such as the scale aggregation model and scale polymorphism are proposed. An important unifying concept in dealing with heterogeneity and integrating ecological and geographical sciences is the invariance of scale. To limit the scale effect, the spatial unit of analysis should be scale-invariant to eliminate spatial heterogeneity and scale dependence. VAU is a spatial unit that is generated from a building cluster without geometric and property heterogeneity. Therefore, the analysis result based on VAU is not related to the spatial resolution of a map or the size. For this reason, we think VAU as a scale invariant analysis spatial unit. Meanwhile, the shape and size of the VAU are only related to the clusters of footprints of adjacent buildings with similar social functions, which is invariant to scale. Since the VAU is both a collection of buildings and a component of the urban block, it cannot only serve as an intermediate unit between the two scales (i.e., building level and patch level), but it can also combine the spatial features of different scales, for a better analysis. In the following parts, we will describe the generation of the VAU.

2.1.1.1 Adjacent building footprint identification and similarity calculation

To cluster buildings with similar social functions, it is essential first to identify the adjacent building footprints. Considering its high efficiency in describing the spatial proximity relationships of objects (He et al., 2018), the Delaunay graph is employed to identify the adjacent building footprints. The centroids of the building footprints are used to generate the Delaunay graph. In the graph, each edge represents the adjacent relationship between two connected building footprints. To avoid clustering irrelevant building footprints, the edges for which the length is more than 200 m are removed at this stage (Caruso et al., 2017).

Based on the identified adjacency relationship, we can then calculate the shape similarity between these adjacent buildings to further identify the adjacent and similar building footprints. Considering that the building footprints used in this study (i.e., collected from OpenStreetMap (OSM)) are mainly delineated and contributed by volunteers, they usually have noise on the edges, which affects the similarity calculation. To overcome this problem, the turning function (TF) method (Arkin et al., 1991) is chosen for the similarity calculation of adjacent buildings. The TF method is widely used for shape

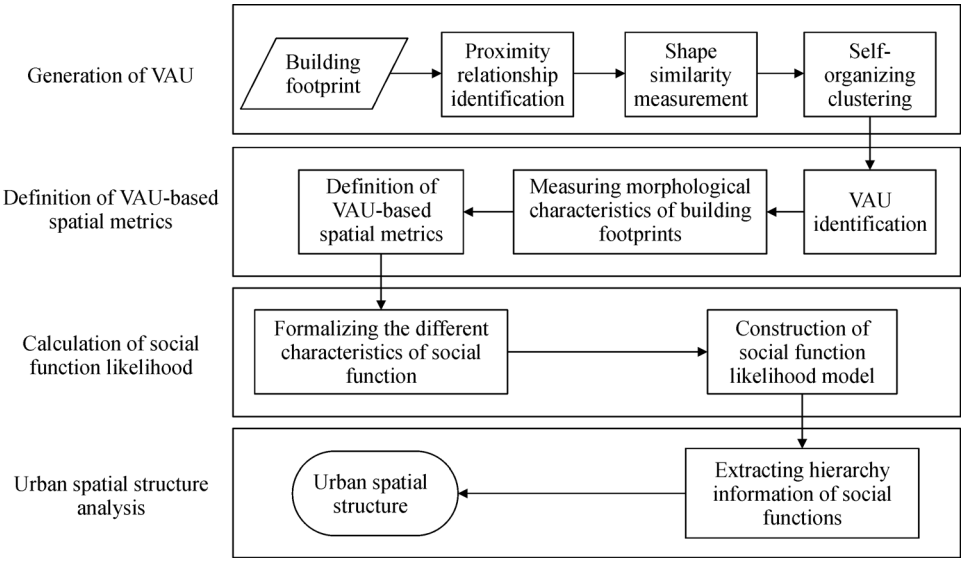

Fig. 1 The pipeline of the proposed approach.

matching and comparison, and is more robust to contour noise than other graph comparison methods (Fan et al., 2014). The main idea of the TF method is to transform a polygon shape from Euclidean space to TF space, which represents a shape using a list of angle-length pairs, as shown in Fig. 2. The angle at a vertex is the accumulated tangential angle at this point, while the corresponding length is the normalized accumulated length of the polygon sides up to this point. Taking Fig. 2(a) as an example, at the start point, the accumulated tangential angle is $\theta_1 = T_1$ and the accumulated length is $S_1 = \frac{L_1}{L_{\text{total}}}$. Along the contour of the polygon in a counter-clockwise direction, θ_i can be calculated as $\theta_i = \alpha \times T_i + \theta_{i-1}$, while the coefficient α is set to -1 for a concave vertex and 1 for a convex vertex. The according accumulated length S_i can be calculated as $S_i = \frac{\sum L_i}{L_{\text{total}}}$. In Fig. 2(b), the horizontal axis represents the normalized perimeter of the polygon, and the vertical axis is the accumulated turning angle according to the edge.

The original TF method, however, can lead to an inconsistent description for the same polygon when its orientation is changed, an example of which is shown in Fig. 3. This can cause the matching results for two similar polygons to be affected by their orientation. One solution is to rotate the polygon and obtain its TF descriptions at different orientations, and then to use these different TF descriptions to derive the minimum shape distance (i.e., the similarity measure) with the other shapes. However, this can greatly increase the computational cost. Another limitation of the TF method is that it cannot be used for cross-comparison, as two sample shapes may have the same shape distance to a reference shape, but it cannot determine if the two sample shapes are similar.

To overcome the aforementioned limitations of the traditional TF method, we make two improvements. To eliminate the description variation caused by the orientation change, we directly use the angle between the initial edge and its adjacent edge as the initial angle θ_1, instead of using the tangential angle. As shown in Fig. 4, after the adjustment of the initial angle θ_1, the TF description for the same polygon is consistent despite the orientation being changed. Hence, the shape distance of the improved TF between two polygons A and B can be simply calculated as follows:

$$d_2(A,B) = \|\Theta_A - \Theta_B\| = \left(\min_{t\in(0,1)} \int_0^1 |\Theta_A(s+t) - \Theta_B(s)|^2\right)^{\frac{1}{2}}, \quad (1)$$

where $\Theta_A(s)$ and $\Theta_B(s)$ are the TF representations of

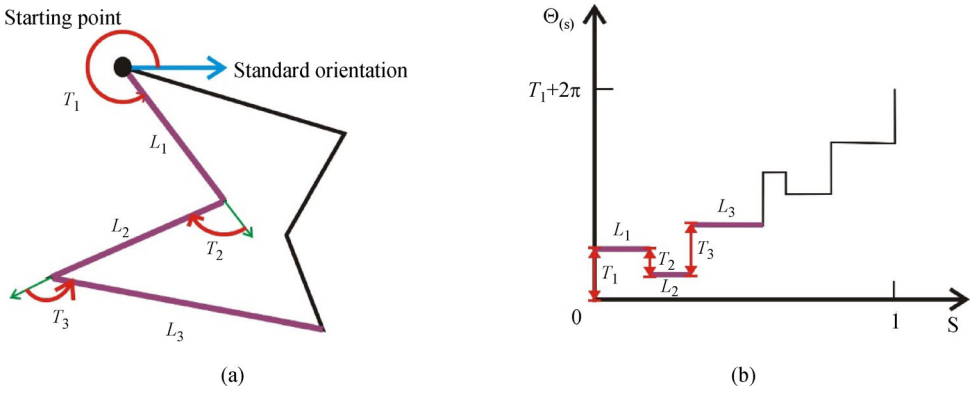

Fig. 2 The transformation from Euclidean space to TF space. (a) Calculation of the accumulated tangential angle and the normalized accumulated length for each vertex of a polygon shape; (b) transformation of the original polygon shape into TF space.

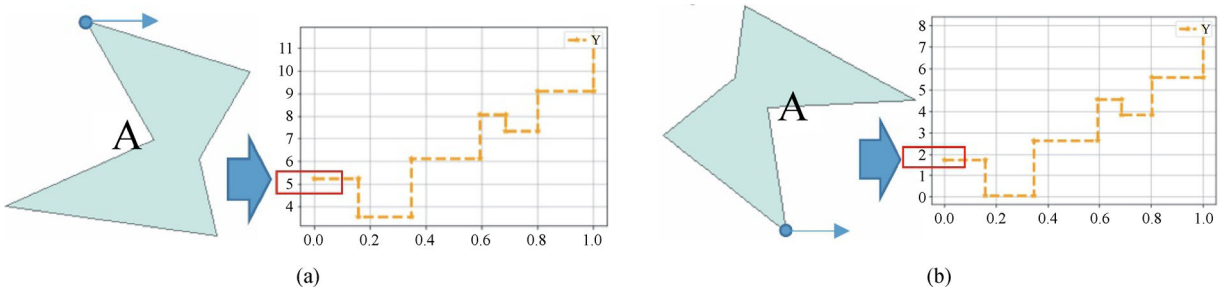

Fig. 3 The effect of polygon rotation on the initial tangential angle. (a) Before rotation; (b) after rotation. With the rotation of the shape, the TF representation is also changed.

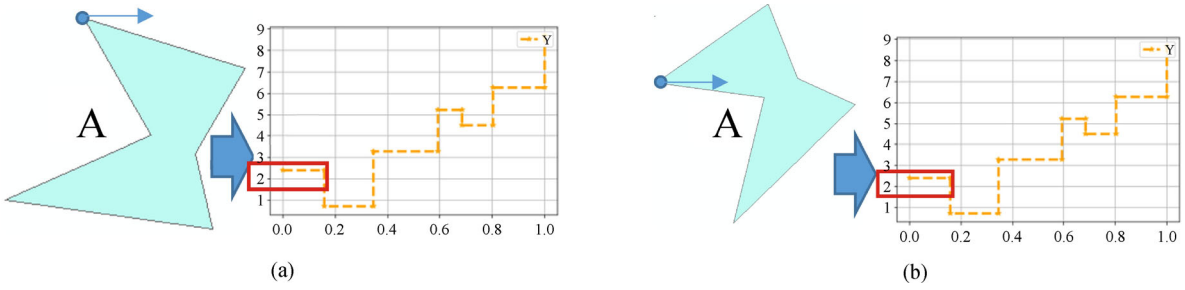

Fig. 4 An invariable initial tangential angle by the improved TF method. (a) TF representation before rotation. (b) TF representation after rotation.

polygons A and B, and $\Theta_A(s+t)$ is the result of the $\Theta_A(s)$ shifting reference point on the boundary of polygon A by moment t.

Furthermore, to facilitate the capability of the TF method for cross-comparison, we convert the shape distance into a shape similarity index, which is a subtraction result from 1 and the dissimilitude. The dissimilitude is defined as the ratio of the shape distance of the two polygons to the average envelope area of the two polygons in TF space. The shape similarity index $\text{similarity}_{A,B}$ of two polygons A and B is formulated as follows:

$$\text{Similarity}_{A,B} = 1 - \frac{d_2(A,B)}{(\text{Envelope\_area}_A + \text{Envelope\_area}_B)/2}, \quad (2)$$

where $d_2(A,B)$ is the shape distance between polygons A and B. Envelope_area is the envelope area of a polygon shape in TF space, which can be calculated as follows:

$$\text{Envelope\_area} = \sum_{i=0}^{n-1} \Theta(s_i) \times (s_{i+1} - s_i) - \min_{t \in (0,1)} \left(\Theta(s_t)\right), \quad (3)$$

where $\Theta(s_i)$ is the accumulated tangential angle corresponding to the accumulated length s_i. Taking polygons A and B as an example, the envelope area of the two polygon shapes is shown in Fig. 5. The shape similarity index can be considered as a normalized distance, which directly gives the similarity degree of the two polygon shapes rather than a simple distance value. It can be used for cross-comparison, dependent on the fact that if two polygon shapes are similar to a sample shape, then these two polygon shapes are also similar.

2.1.1.2 Self-organizing clustering

With the extracted building adjacency relationships and their similarity measurements, a self-organizing clustering algorithm is then used to generate the proposed VAUs. This self-organizing clustering method takes both the building adjacency relationship and shape similarity into consideration, and thus is more adaptable for complex urban scenarios with diverse buildings and varied layouts. The main idea of this algorithm is to iteratively use the adjacent and similar polygons as the follow-up search center. The whole clustering process is done without predefining the number of classes, and the clusters can expand and grow from a randomly selected polygon to the whole input polygons. Thus, we term it "self-organizing clustering". The pseudocode of the algorithm is given below:

Taking Fig. 6 as an example, there are seven polygons involved in the polygon list in this case. The clustering is assumed to start from polygon A. Meanwhile, polygon A is the initial element of the cluster center list of the first

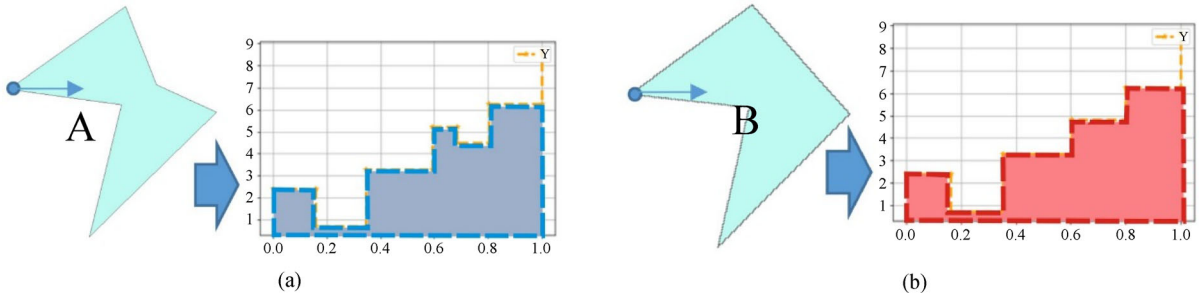

Fig. 5 The envelope area of the TF curve of polygons (a) A and (b) B.

Table 1 Pseudocode of the algorithm

Algorithm 1: Self-organizing clustering

input : Shapefile of building footprints
output: Clusters of building footprint

```
initialization: ClusterList = Null;
for i ← 1 to l do
    // l is the number of polygons in shapefile
    Union (ClusterList, Polygons_i)
    AdjacentPolygons ← FinddAdjacent (polygon_i)
    if AdjacentPolygons not Null then
        for j ← 1 to w do
            // w is the number of adjacent polygons of
               polygon_i
            if edge_{i,j} < 200 m then sim_{i,j} ←
              MeasureSim(polygon_i,AdjacentPolygons_j)
                if sim_{i,j} < 0.9 then
                  Union(ClusterList,AdjacentPolygons_j);
                else continue;
            end
        end
    end
end
```

cluster. The similarity measures are then calculated between A and its identified adjacent polygons B, E, and D. In this study, the similarity threshold was set to 0.9, which means that the adjacent polygon pairs with a similarity measure larger than 0.9 are clustered into the same class. In the case of Fig. 6(a), the similarity measures S(A,B), S(A,D), and S(A,E) are all smaller than the threshold. Hence, there is no cluster generated with polygon A, and A is labeled as a discarded shape and is ignored in the subsequent clustering process. The clustering process is then restarted with polygon B, and the similarity measures are calculated between polygon B and its identified adjacent polygons C, E, and F, as shown in Fig. 6(b). Since the similarity measures S(B,C) and S(B,E) are larger than the predefined threshold, polygons C and E are selected as candidate cluster centers for the following clustering process, as depicted in Fig. 6(c). In Fig. 6(d), the candidate cluster center C and its only adjacent polygon F have a similarity smaller than 0.9, so the self-organizing clustering for center C is terminated. Similarly, the similarity measures between candidate cluster center E and its adjacent polygons D, F, and G are all smaller than 0.9, so the self-organizing clustering for center E is also terminated, as indicated in Fig. 6(e). Consequently, the cluster, which consists of polygons B, C, and E, is generated. In this way, the clustering can be iteratively performed for polygons D, G, and F and expanded to the rest of the input polygons. Based on the proposed self-organizing clustering, all the polygons that meet the requirements of the VAU definition are clustered into a specific class.

To effectively express the form and influence range of the obtained building clusters, we adopt a minimum convex polygon (MCP) estimation for the generation and representation of the VAU, as shown in Fig. 7. For the first step, the clustered building footprints are converted into a set of vertices, as shown in Figs. 7(a) and 7(b). Subsequently, a convex hull algorithm (Getz and Wilmers, 2004) is adopted to compute the MCP of a set of vertices.

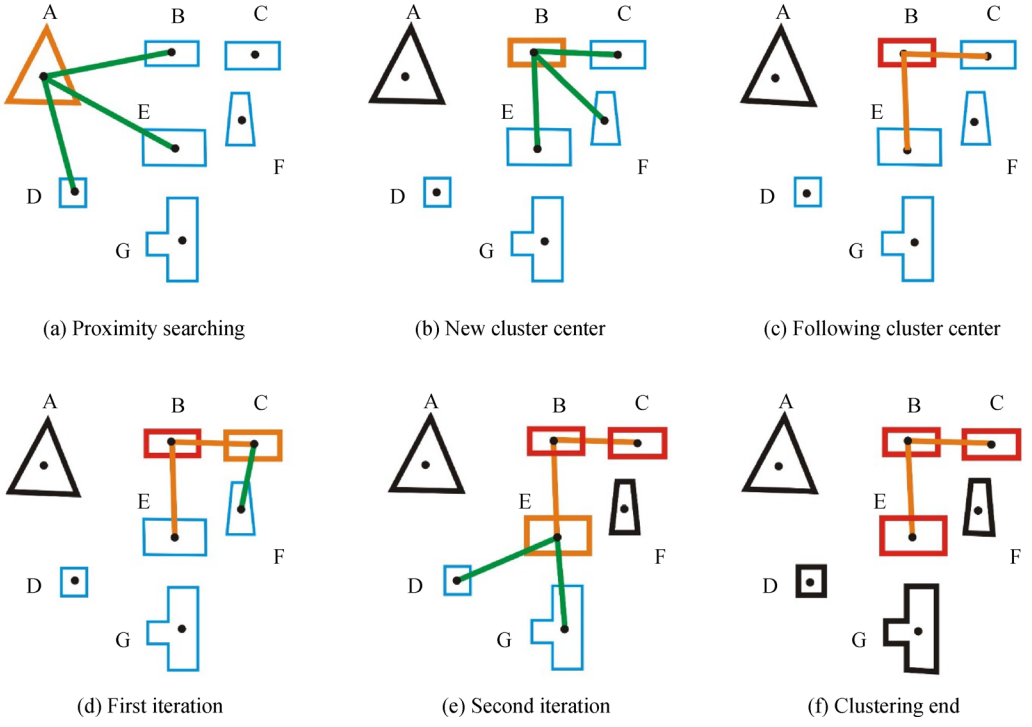

Fig. 6 The self-organizing clustering process for building footprints. The search center is highlighted by the orange border. The green edges represent the proximity relationship. The red border depicts the clustered polygons, while the black represents the unclustered polygons. The orange edges determine the subsequent search center.

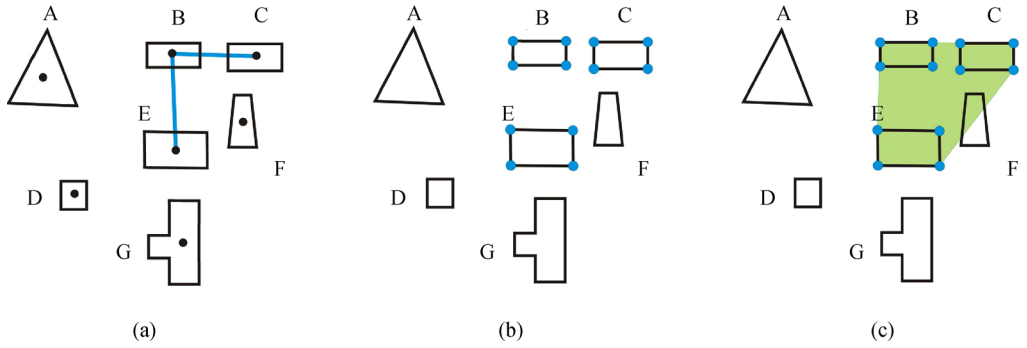

Fig. 7 VAU generation by the vertices of MCP. (a) The clustered building footprints connected by blue lines. (b) The vertices (blue points) of the polygons. (c) The MCP of the vertices set.

Therefore, the VAU is regarded as the convex combination of the vertices of the building footprints in a cluster (Fig. 7(c)).

2.1.2 Definition of VAU-based spatial metrics

The morphological characteristics and spatial distribution pattern of an urban block are usually determined by both the buildings and the built-up area inside this area. However, the existing spatial metrics used for quantifying urban block characteristics are usually independently designed for either the building scale or the patch scale. The inconsistent results obtained by using spatial metrics of different scales may lead to analysis uncertainty. To address this problem, we further present a series of VAU-based spatial metrics, based on the generation of homogeneous VAUs as the spatial units. We first present two spatial metrics — the homogeneity of building orientation (HBO) and the building compactness index (CTI) — which can reflect the orientation and density of buildings in an VAU. These spatial metrics are further used as the basis to construct the VAU-based spatial metrics that describe the spatial arrangement and the composition of the different elements that constitute a block. Since the generated VAU is an intermediate unit between individual buildings and built-up area, the designed spatial metrics are capable of fusing both the local morphological characteristics and the global morphological characteristics in an urban block.

2.1.2.1 Definition of the HBO and CTI

The existing spatial metrics pay more attention to the geometric characteristics, whereas the morphological characteristics (e.g., building orientation and density) are rarely considered. Actually, the building orientation implies the arrangement and interaction of the neighborhood buildings, which is one of the most intuitive morphological features. To quantitatively measure such a characteristic, the HBO metric, which is derived from the Moran's I index, is proposed. The HBO is defined as the weighted result of the difference between the mean and a variable at a building orientation and the same difference for all the other observations in the VAU. The HBO can be calculated by Eq. (4):

$$\mathrm{HBO}_k = \frac{\sum_i \sum_j w_{ij} |Z_j - Z_{\mathrm{ave}}||Z_i - Z_{\mathrm{ave}}|}{\sum_i (Z_i - Z_{\mathrm{ave}})^2}, \tag{4}$$

where Z_i and Z_j are, respectively, the i-th and j-th building orientation angle between the main direction of the building footprint and the x-axis orientation; Z_{ave} is the average orientation angle of all the building footprints in the VAU; and w_{ij} is a weighting parameter. The weighting parameter for the HBO is determined by the inverse distance weighting (IDW) algorithm. To facilitate comparison, the range of the HBO (Eq. (4)) is normalized from 0 to 1. In an VAU, if all the buildings are in the same orientation, the HBO value is 1. Some examples are shown in Fig. 8.

The density and closeness of neighborhood buildings are important indicators of building spatial form in scale-space. In this work, we present the building compactness index (CTI) to represent the density and closeness of the buildings inside an VAU. The CTI is defined as the ratio of the sum area of the building footprint to the area of the VAU, which quantifies the degree of compactness of the buildings in a VAU. It can be calculated by Eq. (5):

$$\mathrm{CTI}_k = \frac{\sum_{i=0}^{n} \mathrm{building\_footprint\_area}_i}{\mathrm{area}_k}, \tag{5}$$

where area_k is the area of the VAU, and $\mathrm{building\_footprint\_area}_i$ is the area of the i-th building footprint in the VAU. The range of the CTI is from 0 to 1. A smaller value of CTI indicates a lower building density and a higher open space ratio, and a higher value of CTI is the opposite.

2.1.2.2 Definitions of the five VAU-based spatial metrics

Cities are planned and built over time, during which built-up areas are formed with varied morphological characteristics. The VAU can outline the exterior of these built-up

areas. Hence, the exploring of the spatial morphological characteristics of VAUs is significant and meaningful for the spatial structure analysis of an urban block. For the quantitative evaluation and analysis of these morphological characteristics, five VAU-based spatial metrics were designed in this study: homogeneity of block (HOB), closeness of block (COB), coverage of VAU (COV), building area entropy of VAU (EOV), and the regularity index (RI). These spatial metrics can quantitatively reflect the topological form and distribution pattern of an urban block. Some examples are shown in Fig. 9.

Many of the spatial metrics have focused on the geometric properties of buildings and have disregarded the topological form information in an urban block (Xing

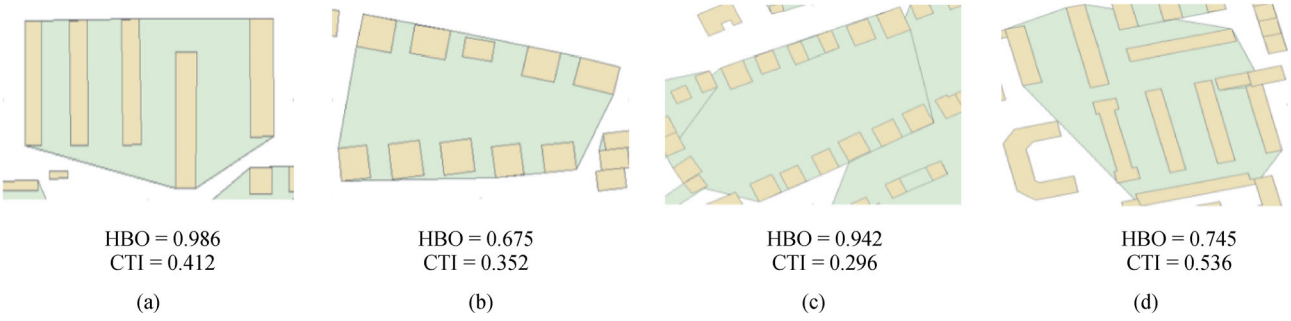

Fig. 8 Examples of HBO and CTI measurement for VAUs with different building orientations and densities.

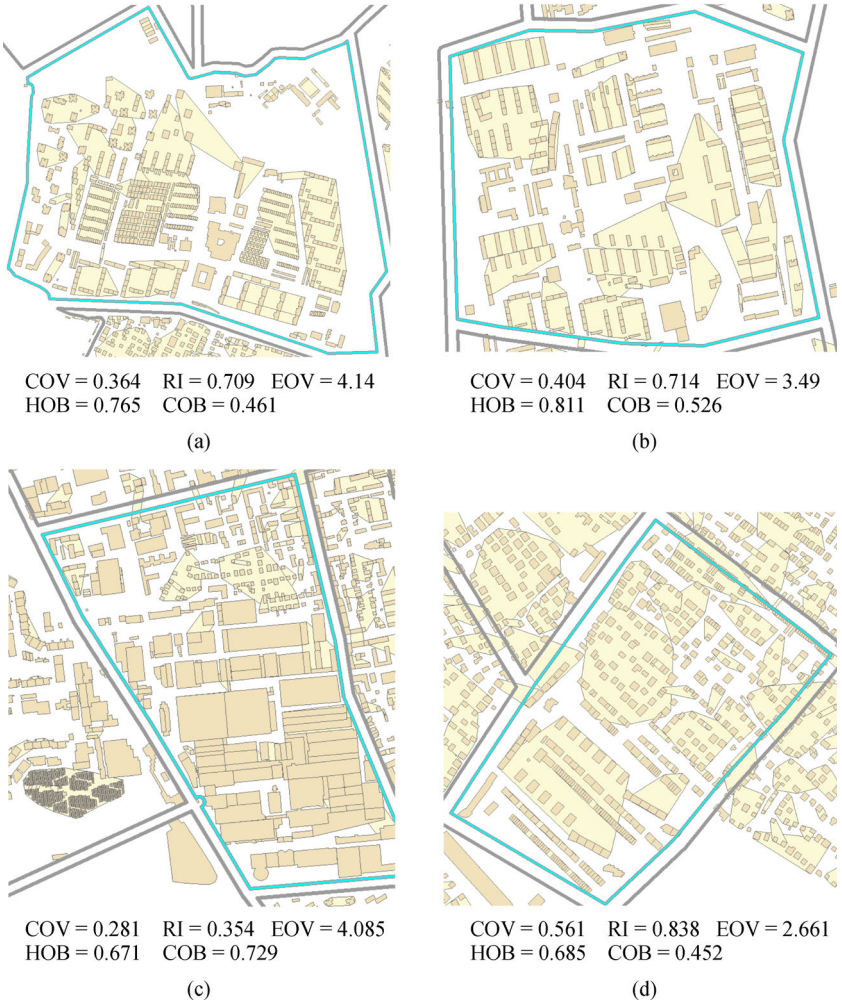

Fig. 9 Examples of VAU-based spatial metrics measurement for VAUs with different spatial morphological characteristics.

and Meng, 2020). To measure the topological relationship between the built-up areas in an urban block, the two aforementioned spatial metrics — HBO and CBO — are employed to formulate the HOB and COB spatial metrics. The HOB is defined as the weighted average of the HBO of all the VAUs in a block, which reflects the order degree of the building orientation in the block. Meanwhile, the COB is defined as the weighted average of the CTI, which reflects the degree of compactness of the built-up areas in a block. The two spatial metrics — HOB and COB — are represented as follows:

$$\mathrm{HOB} = \frac{\sum_{i=1}^{NOM} W_i \times \mathrm{HBO}_i}{\mathrm{NOM}}, \tag{6}$$

$$\mathrm{COB} = \frac{\sum_{i=1}^{NOM} W_i \times \mathrm{CTI}_i}{\mathrm{NOM}}, \tag{7}$$

where *NOM* is the number of VAUs in a block, and HBO_i is the homogeneity of the building orientation of the *i*-th VAU in the block. The CTI_i is the compactness index of the *i*-th VAU in the block, while W_i is the ratio of the area of the *i*-th VAU to the sum of the area of all the VAUs in a block. If the HOB value is close to 1, the block will be close to a linear or grid topology. If the COB value is close to 1, the buildings in the block will exhibit an adjacent topological relationship, and vice versa, in that the opposite will be a separate topological relationship.

In addition to spatial metrics for measuring the topological relationship between built-up areas, we also developed three spatial metrics to measure the spatial configuration of an urban block, which are the coverage of the VAU (COM), the building area entropy of the VAU (EOM), and the regularity index, respectively. The COM metric is the ratio of the built-up area identified by the VAUs in a block to the total floor area of a block, which can be computed as follows:

$$\mathrm{COV} = \frac{VA}{BA}, \tag{8}$$

where *VA* is the sum area of all the VAUs in the block. *BA* is the total area of the block. The COV metric is used to measure the degree of building uniformity in a block. Well planned areas, such as communities and campuses, in which the buildings present good uniformity, will have high COV values.

As important spatial configuration information, the regularity degree of buildings in a block can be measured by the RI metric, which is defined as the ratio of the number of buildings contained in the homogeneous VAUs to the total number of buildings in a block:

$$\mathrm{RI} = \frac{NB}{SB}, \tag{9}$$

where *NB* is the number of the building footprints contained in an VAU, and *SB* is the sum of all the buildings in the block. A higher value of RI indicates a more regular and uniform building distribution in a block.

Buildings with different social functions often have different types of building footprints. The mixture degree of building footprints in an urban block reflects its spatial configuration complexity with respect to the different social functions. However, it is difficult to directly measure this complexity. Since the different types of buildings have different floor areas, the floor area, in turn, indicates the type of building. Considering that a VAU is a homogenous spatial unit (i.e., the buildings inside an VAU are adjacent and similar), the average area of the VAU is thus an indication of the type of buildings inside the VAU, as well as the social function configuration of that VAU. The average floor area of the overall VAUs is divided into n levels. The spatial configuration complexity of an urban block is then measured by the mixture degree of the different levels of the average floor area of the VAUs. Specifically, the spatial metric for measuring this complexity can be formulated as the following entropy calculation problem:

$$\text{The building area entropy of VAU(EOV)} = -\sum_{k=1}^{10} P_k \log P_k, \tag{10}$$

where p_k is the ratio of the number of VAUs with the average floor area belonging to the *k*-th level to the total number of VAUs in an urban block. A high value of EOV indicates a more complex spatial configuration of a block (with more social function types).

2.1.3 Calculation of the social function likelihood

The calculation of the social function likelihood for each urban block is an essential ingredient to accomplish social function identification. The three different social functions (i.e., residential, industrial, commercial) show different morphological and geometrical characteristics. Studies have shown that four to six spatial metrics are sufficient to express the differences between the three types of social functions (Herold et al., 2003b). The buildings in a residential area usually have an orderly arrangement and a dense spatial distribution, and most residential buildings have a simple geometry with a small floor area. The floor area of workshop is much larger than the floor area of house and shopping mall. Although these industrial buildings have a large distance from each other, these buildings still present a regular arrangement. The buildings in a commercial area distribute with a low regularity and with more compactness. Most shopping malls and office buildings have a complex geometry with a large building footprint. A comparative analysis of the different characteristics of the three types of functional zones is shown in Table 2.

Table 2 Characteristics of each functional zone

Social function	Architectural characteristics	Spatial distribution characteristics	Spatial metrics
Residential	Simple shape, uniform size	Regular, high building density	COV,RI,HOB,BD,EOV
Industrial	Rectangular shape, large size	Well organized, low building density	COV,HOB,BS,TOM,BD
Commercial	Complex shape, large size	Disordered, high building density	EOV,CI,TOM,BS,RI

In Table 2, the BD metric is the density of the building footprints (Galster et al., 2001), while CI is the average compactness index of the building footprint shapes in a block (Huang et al., 2007). The BS metric is the mean building size in a block (Herold et al., 2003a). In this study, for each type of social function, the five spatial metrics with the highest positive or negative correlation were selected to construct the social function likelihood models. Taking both the architectural characteristics and spatial distribution characteristics into consideration, we assemble the proposed VAU-based spatial metrics with the two existing applicable spatial metrics to formulate better models for calculating the social function likelihood of each urban block:

$$\begin{aligned}\text{Residential}_i = {} & w_i^{\text{COV}} \times \text{COV}_i + w_i^{\text{RI}} \times \text{RI}_i + w_i^{\text{HOB}} \\ & \times \text{HOB}_i + w_i^{\text{BD}} \times \text{BD}_i - w_i^{\text{EOV}} \\ & \times \text{EOV}_i, \end{aligned} \tag{12}$$

where Residential_i denote the residential likelihood value of the i-th urban block belonging. W_i^* is the weight for the corresponding spatial metric of the i-th urban block. In each equation, a spatial metric with a positive correlation with that type of function will have a positive weight; otherwise, it will have a negative weight.

$$\begin{aligned}\text{Industrial}_i = {} & w_i^{\text{COV}} \times \text{COV}_i + w_i^{\text{HOB}} \times \text{HOB}_i \\ & + w_i^{\text{COB}} \times \text{COB}_i + w_i^{\text{BS}} \times \text{BS}_i - w_i^{\text{BD}} \\ & \times \text{BD}_i, \end{aligned} \tag{13}$$

where Industrial_i denote the industrial likelihood value of the i-th urban block belonging.

$$\begin{aligned}\text{Commercial}_i & \\ = {} & w_i^{\text{EOV}} \times \text{EOV}_i + w_i^{\text{CI}} \times \text{CI}_i + w_i^{\text{COB}} \times \text{COB}_i \\ & + w_i^{BS} \times BS_i - w_i^{\text{RI}} \times \text{RI}_i, \end{aligned} \tag{14}$$

where Commercial_i denote the likelihood value of the i-th urban block belonging to the three types of social functions. $\text{Spatial Metric}(*)_i$ denotes the spatial metric measured on the i-th urban block. For each spatial metric, it can obtain an ascending order according to the value measured on all the urban blocks. For function likelihood models, the weight value of a specific spatial metric $w_i^{\text{Spatial Metric}(*)}$ for the i-th urban block can be calculated as follows:

$$w_i^{\text{Spatial Metric}(*)} = \frac{o_i^*}{\sum_{j=1}^{5} o_i^j}, \tag{15}$$

where O_i^* is the sorting result of the i-th urban block for a specific spatial metric. Where O_i^j is the sorting result of the i-th urban block for the j-th specific spatial metric of a functional likelihood function.

2.2 Social function likelihood-based urban spatial structure analysis

Urban blocks have usually been assumed to be of a single social function type. Their spatial configuration and distribution are then used for the urban spatial structure analysis (Walde et al., 2014). However, as mentioned in the Introduction, the social functions of an urban block can be more complex and diverse, which means that an urban block usually has mixed social function types. Hence, the use of urban units identified with a single social function type to describe and analyze urban spatial structure is not accurate. In this study, we instead used the spatial distribution pattern and development trends of the social functions themselves in a city to undertake the urban spatial structure analysis. A spanning tree approach was employed to extract the hierarchical information of the spatial distribution and the development trends of the urban social functions, to reveal the development discrepancies and the interactions of neighborhood blocks with respect to the different social functions.

The hierarchical information of urban social functions residing in the relations of neighborhood urban blocks is another aspect that can be used to reveal the spatial distribution characteristics and development trends of urban social functions. In our study, since the spanning tree approach is an effective way to generate a structural representation of graphical shapes, the minimum spanning tree (MIST) and the maximum spanning tree (MAST) were employed to extract the hierarchical information of the urban social functions. First, the centroids of all the urban blocks were used as the vertices to construct the Delaunay triangulation. Thus, each Delaunay edge connects two

neighborhood urban blocks, and each edge is assigned with three weights. The weights are the difference of three social function likelihoods between the two neighborhood blocks. Consequently, for each type of social function, the MIST and MAST can be applied to generate the social function difference graph based on this weighted Delaunay triangulation. The MIST of the social function difference graph is a connected graph with the minimum total edge weights, while the MAST of the social function difference graph is a connected graph with the maximum total edge weights. Here, for simplicity, we refer to them as DMIST and DMAST.

3 Experimental results

In this study, the OSM building footprints for 25 boroughs of the city of Munich in Germany were used for the testing. The study site included 158767 building footprints, with an area close to 310 km^2. Moreover, the urban area was divided into 371 city blocks, according to the main street network of OSM.

3.1 Urban social function identification results for Munich

To identify the social function types of the 371 urban blocks of Munich, the self-organizing clustering method was first applied to generate the VAUs for all the input building footprints. The number of final generated VAUs was 20400, covering about 72% of the input footprints.

With the obtained VAUs, the five developed spatial metrics were then utilized to measure the morphological characteristics of each VAU. The results are displayed in Fig. 10, which shows an obvious difference in the morphological characteristics of the buildings between the urban area and suburban area.

Figure 10(a) shows that the urban blocks near the trunk roads show high HOB values, which is consistent with the real situation of the buildings near these areas having a similar orientation. In Fig. 10(b), the COB values show large differences between the urban blocks in the center and in the suburban area of Munich, which can be attributed to the fact that the buildings in the center of the city are more densely distributed, while the buildings in the suburban area of the city are relatively sparsely distributed. From Figs. 10(c) and 10(d), it can be seen that the urban blocks near the center of Munich generally have lower COV and RI values, while the suburban areas, especially in the east and southwest of Munich, have relatively high COV and RI values. The results imply that the buildings near the city center have large shape differences and a disordered spatial layout. In contrast, buildings in the built-up areas to the east and southwest of the city are well ordered and configured more homogeneously. Moreover, in the west and south of Munich, the buildings have more spatial types, and the urban blocks take on diverse social functions, while the high EOV derived by our method in Fig. 10(e) also validates this finding.

The social function likelihoods concerning the three types of social functions were calculated for the 371 urban blocks of Munich, using the models presented in Section 2.1.3. For the convenience of the following analysis and comparison, the social function likelihoods with respect to the three types of social functions are referred to as the commercial function likelihood, the industrial function likelihood, and the residential function likelihood, with all the calculated values normalized to 0 to 1. Using 0.2 as the interval, a statistical analysis for the number of blocks with a function likelihood belonging to a certain value range with respect to the three types of functions is provided in Table 3. Blocks with one of the three function likelihoods belonging to different value ranges have different potential meanings: 0.8–1.0 indicates that the block is more likely to have a single social function type; 0.6–0.8 indicates that this social function type dominates the block; 0.4–0.6 indicates that the block has mixed social function types and is relatively balanced; 0.2–0.4 indicates that this social function type is auxiliary to that block; and 0.0–0.2 indicates that this social function type is not obvious for that block. For example, the value 107 (~28.9%) in the first row means that there are 107 blocks (nearly 28.9% of the 371 blocks) with a residential function likelihood belonging to the range of 0–0.2, indicating that the residential function is not obvious in these blocks.

From Table 3, it can be found that nearly 70.1% of the blocks have a commercial function likelihood of larger than 0.4, while only 21.2% and 32.2% of the blocks have an industrial or residential function likelihood of larger than 0.4, respectively. These findings imply that the commercial function is more important than the other two social functions. Meanwhile, nearly 63.8% of the blocks have a residential function likelihood of 0.2–0.6, which means that most of the blocks possess a residential function and are relatively balanced. It is not surprising that the industrial function is auxiliary to most of the blocks, since nearly 78.6% of the blocks have an industrial function likelihood of 0–0.4. In addition, blocks with all three function likelihoods belonging to 0.2–0.6 are of a high proportion, which means that most of the blocks have mixed social functions.

The histogram of the distribution of the number of blocks along with the three function likelihoods shown in Fig. 11 also confirms these statements. In Fig. 11(a), the residential function likelihoods for most of the blocks are relatively evenly distributed in the low- and medium-value regions, while only a small number of blocks possess high values. This also reveals that only a few blocks have only a residential function. In Fig. 11(b), a number of blocks with the commercial function likelihood present a negative skewness distribution (i.e., there is some offset in the direction of the high values), indicating that the commercial function dominates a large number of blocks. In Fig.

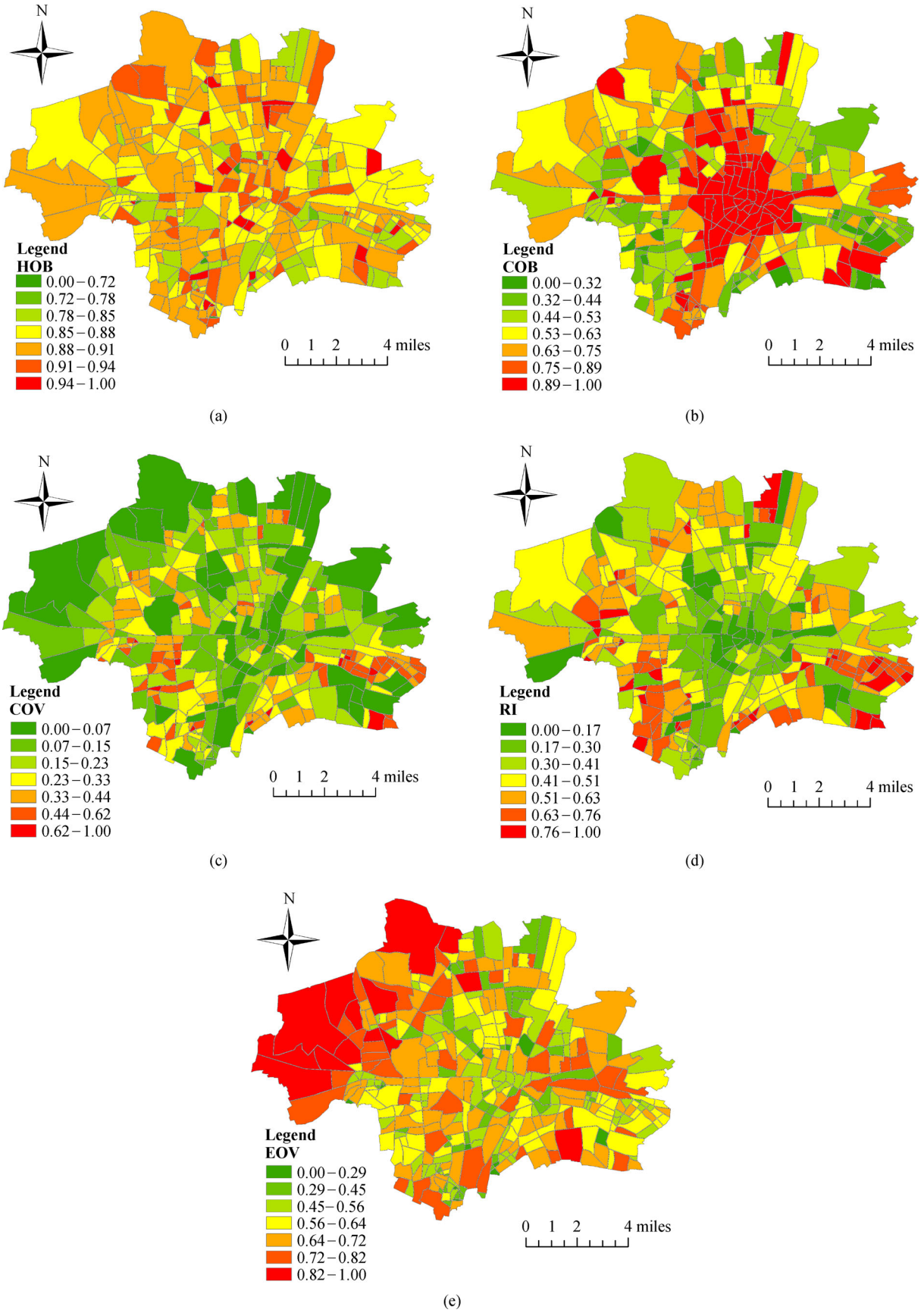

Fig. 10 Spatial distribution of the calculated five VAU-based spatial metric results for the city blocks in Munich: (a) homogeneity of block, (b) closeness of block, (c) coverage of VAU, (d) regularity index, and (e) building area entropy.

Table 3 The three kinds of social function likelihood segmentation statistics

Type	Interval				
	0–0.2	0.2–0.4	0.4–0.6	0.6–0.8	0.8–1
Residential	107 (~28.9%)	144 (~38.8%)	93 (~25%)	21 (~5.6%)	6 (~1.6%)
Commercial	22 (~5.9%)	88 (~23.7%)	112 (~30.1%)	109 (~29.3%)	40 (~10.7%)
Industrial	111 (~29.9%)	181 (~48.7%)	59 (~15.9%)	17 (~4.5%)	3 (~0.8%)

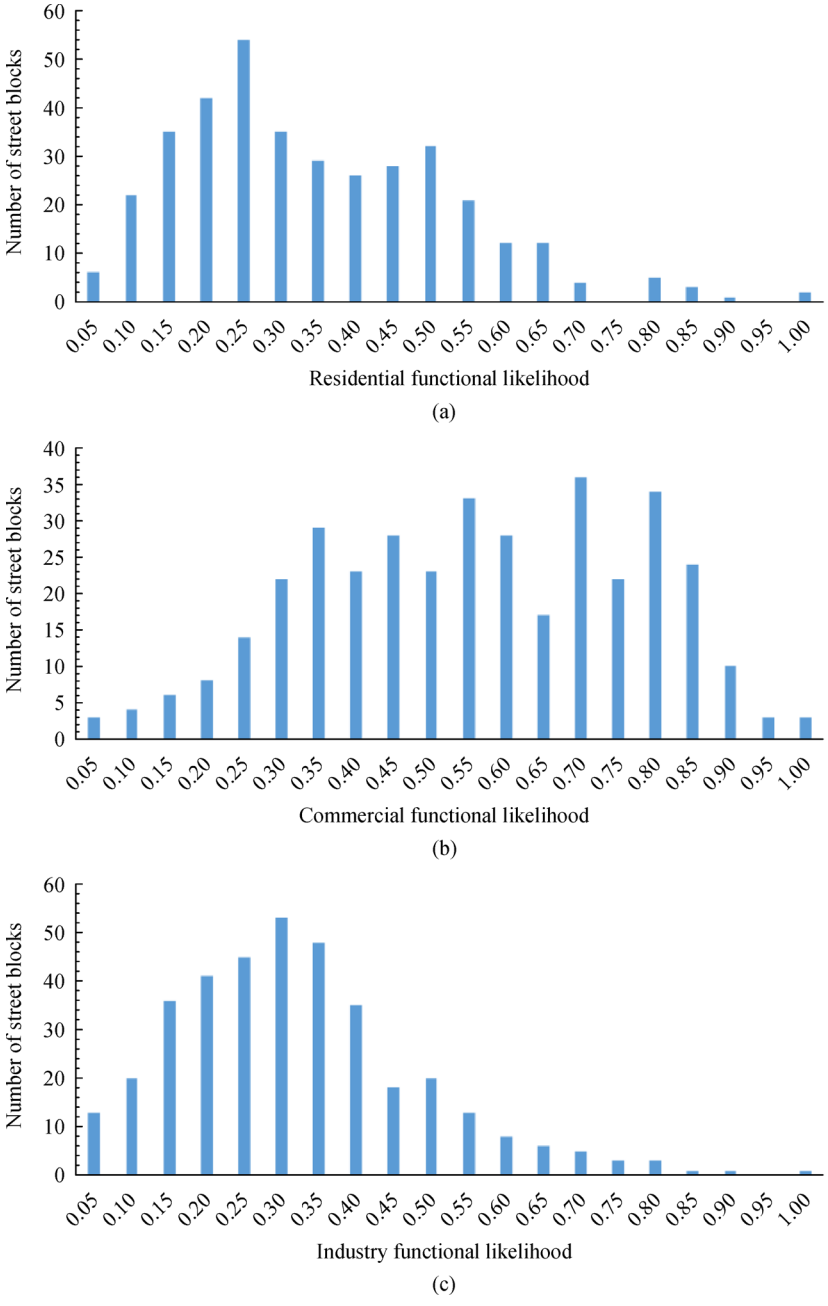

Fig. 11 The distribution of the number of blocks with regard to the three social function likelihood types.

11(c), the blocks with the industrial function likelihood distribute mainly in the medium- and low-value regions, indicating that most of the city blocks have only a weak industrial function.

To demonstrate the effectiveness of social function, we randomly selected 60 sub-sampled blocks for the whole city. Considering the completeness and timeliness of land-use data in Munich, we chose OSM land-use data to be reference data. Test data are the calculated dominating functional type of each street block. To verify the result's correctness, we employ a confusion matrix visualizing the performance of our method (Stehman, 1997). The confusion matrix is a table with three rows and three columns that reports the number of false positives, false negatives, true positives, and true negatives. According to the reference data, for the given sample of 60 areas, 17 sub-sampled blocks belong to the industry function area, 21 sub-sampled blocks belong to the commercial function area, and 22 sub-sampled blocks belong to the residential area. In comparison, the dominating function type is represented as a predicted type. The result of the predicted functional zone type is shown in Table 4.

Table 4 Confusion matrix

Predicted type	Actual type		
	Industry	Commercial	Residential
Industry	14	2	0
Commercial	3	16	4
Residential	0	3	18

We use overall accuracy to show how often our result is corrected. The formula of overall accuracy is expressed as below:

$$\text{Accuracy(ACC)} = \frac{TP + TN}{TP + TN + FP + FN}, \qquad (16)$$

where *TP* is true positive; *FP* is false positive; *TN* is true negative; *FN* is false negative. The result of accuracy is 0.8.

3.2 The spatial structure of Munich with respect to urban social functions

In this section, the urban spatial structure of Munich is analyzed based on the spatial distribution characteristics of the three types of urban social functions. The MIST of the social function difference graph was utilized to extract the hierarchical information of the spatial distribution and the development trends of the urban social functions. The MAST of the social function difference graph was utilized to reveal the development discrepancies and interactions of the neighborhood blocks. The results of DMAST and DMIST generated on the three types of social functions are shown in Fig. 12 and Fig. 13, respectively.

In Fig. 12, according to the weights of the DMIST edges, the Jenks natural breaks approach was employed to classify these edges into high-, mid-, and low-level ones, which are labeled with red, yellow, and blue, respectively. The different levels of edges imply the development hierarchy of the neighborhood blocks with respect to the same social function: a high-level edge (in red) indicates that the two connected neighborhood blocks have large differences in development degree; a mid-level edge (in yellow) indicates that the two connected neighborhood blocks have a moderate difference in development degree; and a low-level edge (in blue) indicates that the two connected neighborhood blocks have similar development degrees. For example, the Schloss Nymphenburg Park has a moderate difference with its adjacent residential districts in residential function, and thus the DMIST edges connecting the corresponding blocks are classified as mid-level edges (in yellow), as highlighted by the black border in Fig. 12(a). The blue edges in the area of Berg am Laim and Trudering-Riem in Fig. 12(b) indicate that the blocks have similar development degrees of commercial function. This is because most of the blocks around these two boroughs are mainly residential areas, and the level of commercial development is generally low. In Fig. 12(c), a representative example reflecting a big gap in the level of industrial development between the two blocks can be found in Bogenhausen, where there are two blocks connected by a red edge.

The DMAST can help us to reveal the interactions of neighborhood blocks in a local region for the different types of social functions. This is done by a local maximum point and local minimum point analysis. For the DMAST of each of the three types of social functions, if a block (a node of DMAST) has a maximum/minimum function likelihood among its neighborhood blocks (connected by DMAST edges), we consider this node to be a local maximum/minimum node with respect to the particular type of social function. As shown in Figs. 13(a)–13(c), the local maximum and minimum nodes, as well as the corresponding edges in the DMAST, are colored in red and blue, respectively. In this study, only nodes with three or more edges were taken into account for the local interaction analysis. The local maximum and minimum nodes have meaningful implications. The local maximum node indicates that the corresponding block has a complementary effect on its neighbors for the particular type of social function. Meanwhile, it also indicates an expansion trend for that type of social function in a local region. In contrast, the minimum node indicates that the corresponding block has a restricting effect on its neighbors, and the respective social function tends to shrink in that local region. For example, in the north of Munich, e.g., the administrative region of Schwabing-Freimann, there are industrial and commercial zones in the corresponding blocks, while blocks which provide a residential function to the factory workers and store clerks

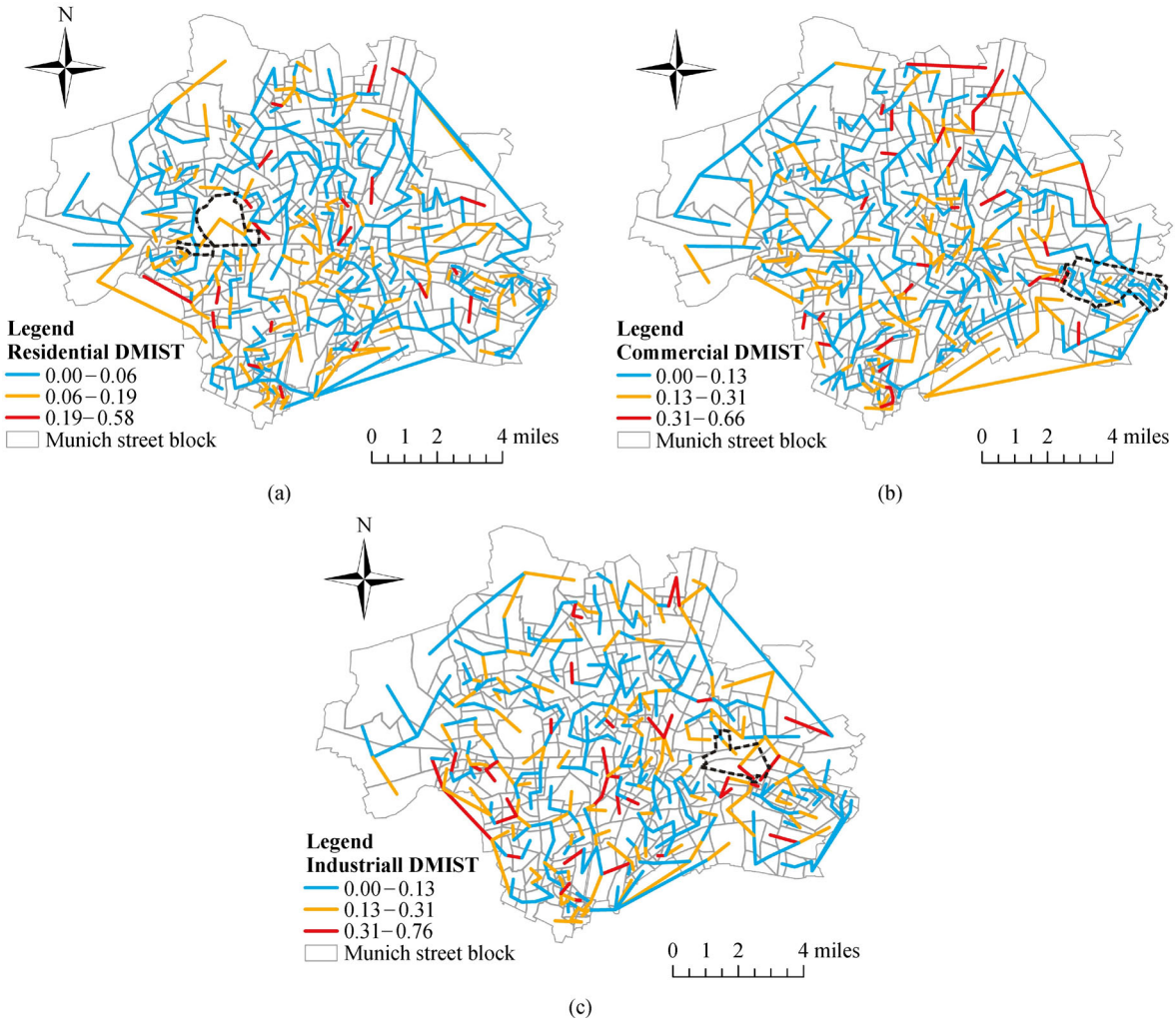

Fig. 12 The DMIST of the social functions. The blue polylines represent the expansion direction, and the yellow and red polylines indicate significant differences in social function: (a) the DMIST of the residential function; (b) the DMIST of the commercial function; (c) the DMIST of the industrial function.

can be found adjacent to these blocks. Hence, the local maximum nodes appear with respect to the residential function, as highlighted by the black border in Fig. 13(a). This in turn demonstrates that the local maximum blocks have a complementary effect on their neighbors for a certain type of social function. In Fig. 13(b), the block where the Alter Nordfriedhof ("Old North Cemetery") is located is occupied by free space, which is very different to the commercial districts in the adjacent Glockenbachviertel. In Fig. 13(c), the Munich railway station is located in the block at the local maximum node. This also proves that the block located at the local maximum node complements the industrial function of the surrounding neighborhood. More interaction information for the neighborhood blocks can also be obtained from Fig. 13 with the help of the DMAST.

4 Discussion and conclusions

4.1 The effectiveness of the VAU-based spatial metrics for expressing the urban form

Spatial metric is an effective tool for describing and measuring the morphological characteristics and spatial configuration of buildings in a city. For a large and complex urban system, the Xing and Meng (2020) chose either patch-level or building-level spatial metrics for the urban analysis. Unfortunately, the results measured with different scales of spatial metrics are usually not relevant to the same research area, as can be seen in Fig. 14. For example, in Fig. 14(a), using the building-level spatial metrics, we can obtain the geometric and topological information of each of the 25 building objects; however,

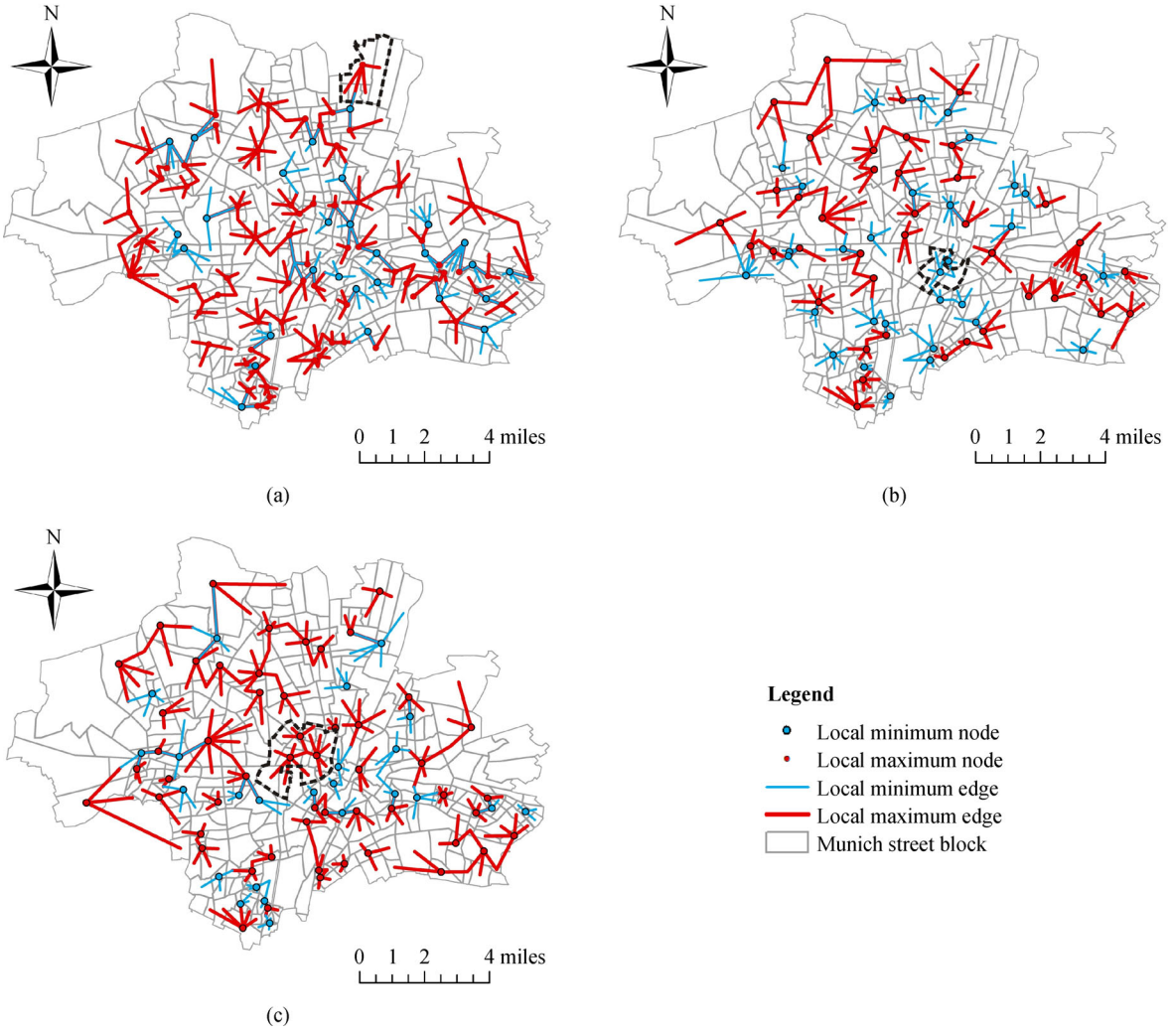

Fig. 13 The DMAST of the social functions. Blue edges represent the restricting effect of the local minimum node to the neighboring blocks; red edges reflect the complementary effect of the local maximum node to the neighboring blocks. (a) The DMAST of the residential function. (b) The DMAST of the commercial function. (c) The DMAST of the industrial function.

the global characteristics of these buildings are absent. In contrast, in Fig. 14(c), the global spatial configuration of the buildings can be well measured. In contrast, the detailed local features are weakened due to the overuse of the averaging operation. Compared with the two aforementioned types of spatial metrics, the proposed VAU-based spatial metrics are better at preserving both the local and global characteristics of building clusters. Since the VAUs are generated from building clusters with high interior homogeneity, the VAU can be considered a favorable intermediate spatial unit that connects the two spatial scales. Hence, the spatial metrics developed based on the VAU are a bridge to the existing spatial metrics designed for different scales, which cannot only alleviate the uncertainty of the urban spatial structure analysis resulting from the scale effect, but can also enrich the urban analysis.

4.2 Toward a function likelihood based approach for depicting spatial structure

The clear identification and description of the social function types of urban blocks is fundamental to urban spatial structure analysis. In this study, we used social function likelihoods to quantitatively describe the membership degree of a block to the three types of social functions, rather than identifying a single social function for each urban block. The computational models for the three types of function likelihoods were constructed based on the specific spatial and morphological characteristics of the different types of social functions. These characteristics can be quantitatively defined and measured by the different spatial metrics, which makes the proposed method more capable of accurately describing the social function types that an urban block would carry. The experimental results

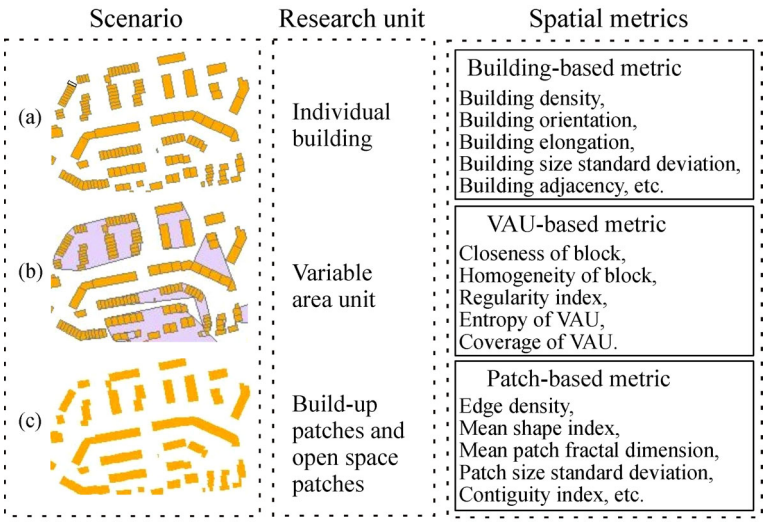

Fig. 14 Spatial metrics designed for three kinds of different object scenarios in the same region. For scenario (a), an individual building is regarded as the research unit. For scenario (b), an VAU is regarded as the research unit. For scenario (c), a patch is regarded as the research unit.

described in Section 3.1 also showed that, by using social function likelihoods, it is possible to quantitatively distinguish the intensity of each type of social function carried by an urban block, for both blocks with mixed social functions and for blocks with a single social function.

The quantitative description of urban social functions with social function likelihoods allows a DMIST and DMAST analysis to be conducted, which provides the structural and hierarchical information of the spatial distribution and the development trends of the social functions for use in urban spatial structure analysis. The DMIST and DMAST analysis cannot only reflect the expansion and constriction trends of urban social functions, but also the relations, the interactions, and the development discrepancies of the neighborhood urban blocks. These results are more intuitive and comprehensive than the urban social function zone distribution maps provided in existing works (Xing and Meng, 2020). From the DMIST and DMAST results described in Section 3.2, it was found that the urban development of Munich is of a sprawl type rather than being based on internal renewal. According to the structural information of the social functions given by the experimental results, people can try to slow down the speed of urban sprawl by adjusting the land-use planning of urban blocks. Meanwhile, the hierarchical information can facilitate the allocation of resources to optimize the development of problematic blocks.

Despite the use of social function likelihoods having many merits in urban spatial structure analysis, it still has some limitations. Since the social function likelihoods are calculated with building footprint data, they may be affected by the quality and completeness of OSM data. Moreover, it should be pointed out that social function likelihoods are relative values (because the weight parameters in the computational models are determined by the overall blocks) that reflect the different social function types and intensities of the different urban blocks in a research area. Thus, changing the size of the study area will lead to changes in the results of the social function likelihood computation. In this case, the social function likelihoods of each urban block should be updated. However, this does not affect the final urban spatial structure analysis result, since social function likelihood is just a proxy for urban social function distribution patterns and development trends.

5 Conclusions

In this paper, we have investigated a method for urban spatial structure analysis based on the exploration of the spatial distribution patterns, development trends, and hierarchical information of urban social functions using building footprint data. Given the fact that the social functions of an urban block can be complex and diverse,

we constructed a set of models to quantitatively calculate the social function likelihoods with respect to the three types of social functions. Compared with the previous works that identified a single social function for each urban block, the use of social function likelihoods can accurately describe the mixture degree of the three types of social functions in a block. Specifically, the computational models for the social function likelihoods in this study were mainly constructed by the proposed VAU-based spatial metrics. These spatial metrics are defined based on the homogeneous VAU as the spatial unit, and are thus

robust to scale and effective at measuring the overall characteristics of an urban block. Hence, the use of urban social function likelihoods for spatial structure analysis is effective and reliable.

6 Further work

The case study conducted for the city of Munich showed that the use of social function likelihoods facilitates the quantitative description of each type of social function that an urban block carries, based on the measurement of the geometric and morphological characteristics, and the spatial configuration of the buildings of an urban block. Based on the social function likelihoods calculated for 371 urban blocks of Munich, the structural and hierarchical information of the urban social functions, as well as the development trends of the different social functions of the city, were detected and analyzed. These diagnostic results for Munich can potentially assistant city planners and policymakers to adjust the formulation of future urban planning, and to achieve sustainable urban development.

Data and codes availability statement The data and codes that support the findings of this study are available in repository "Github" with the identifier at the public link. The authors would like to thank Mr. Karimbahgat and his team for providing the Pyshp (shapefile.py) for reading and writing shapefile. They would also like to thank the OpenStreetMap (OSM) for providing the Munich building footprint data.

Acknowledgments This research was funded by the National Key Research and Development Program of China (No. 2018YFB0505400), and the National Natural Science Foundation of China Project (Grant Nos. 42071370 and 41771484).

References

Anas A, Arnott R, Small K A (1998). Urban spatial structure. J Econ Lit, 36(3): 1426–1464

Arkin E M, Chew L P, Huttenlocher D P, Kedem K, Mitchell J S (1991). An efficiently computable metric for comparing polygonal shapes. IEEE T PATTERN ANAL, 13(3): 209–216

Arnott R (1998). Congestion tolling and urban spatial structure. J Reg Sci, 38(3): 495–504

Boarnet M G, Hong A, Santiago-Bartolomei R (2017). Urban spatial structure, employment subcenters, and freight travel. J Transp Geogr, 60: 267–276

Burgalassi D, Luzzati T (2015). Urban spatial structure and environmental emissions: a survey of the literature and some empirical evidence for Italian NUTS 3 regions. Cities, 49: 134–148

Caruso G, Hilal M, Thomas I (2017). Measuring urban forms from inter-building distances: combining MST graphs with a local index of spatial association. Landsc Urban Plan, 163: 80–89

Chen Y, Liu X, Li X, Liu X, Yao Y, Hu G, Xu X, Pei F (2017a). Delineating urban functional areas with building-level social media data: a dynamic time warping (DTW) distance based *k*-medoids method. Landsc Urban Plan, 160: 48–60

Chen Z, Yu B, Song W, Liu H, Wu Q, Shi K, Wu J (2017b). A new approach for detecting urban centers and their spatial structure with nighttime light remote sensing. IEEE Trans Geosci Remote Sens, 55(11): 6305–6319

Ding C, Zhao X (2014). Land market, land development and urban spatial structure in Beijing. Land Use Policy, 40: 83–90

Fan H, Zipf A, Fu Q, Neis P (2014). Quality assessment for building footprints data on OpenStreetMap. Int J Geogr Inf Sci, 28(4): 700–719

Galster G, Hanson R, Ratcliffe M R, Wolman H, Coleman S, Freihage J (2001). Wrestling sprawl to the ground: defining and measuring an elusive concept. Hous Policy Debate, 12(4): 681–717

Getz W M, Wilmers C C (2004). A local nearest-neighbor convex-hull construction of home ranges and utilization distributions. Ecography, 27(4): 489–505

Gordon P, Kumar A, Richardson H W (1989). The influence of metropolitan spatial structure on commuting time. J Urban Econ, 26(2): 138–151

Grippa T, Georganos S, Zarougui S, Bognounou P, Diboulo E, Forget Y, Lennert M, Vanhuysse S, Mboga N, Wolff E (2018). Mapping urban land use at street block level using OpenStreetMap, remote sensing data, and spatial metrics. ISPRS Int J Geoinf, 7(7): 246

He X, Zhang X, Xin Q (2018). Recognition of building group patterns in topographic maps based on graph partitioning and random forest. ISPRS J Photogramm Remote Sens, 136: 26–40

Heiden U, Heldens W, Roessner S, Segl K, Esch T, Mueller A (2012). Urban structure type characterization using hyperspectral remote sensing and height information. Landsc Urban Plan, 105(4): 361–375

Herold M, Goldstein N C, Clarke K C (2003a). The spatiotemporal form of urban growth: measurement, analysis and modeling. Remote Sens Environ, 86(3): 286–302

Herold M, Liu X, Clarke K C (2003b). Spatial metrics and image texture for mapping urban land use. Photogramm Eng Remote Sensing, 69(9): 991–1001

Hermosilla T, Palomar-Vázquez J, Balaguer-Beser Á, Balsa-Barreiro J, & Ruiz L A (2014). Using street based metrics to characterize urban typologies. Comput Environ Urban Syst, 44: 68–79

Huang B, Zhao B, Song Y (2018). Urban land-use mapping using a deep convolutional neural network with high spatial resolution multi-spectral remote sensing imagery. Remote Sens Environ, 214: 73–86

Huang J, Lu X X, Sellers J M (2007). A global comparative analysis of urban form: applying spatial metrics and remote sensing. Landsc Urban Plan, 82(4): 184–197

Joh C H, Hwang C A (2010). A time-geographic analysis of trip trajectories and land use characteristics in Seoul metropolitan area by using multidimensional sequence alignment and spatial analysis. In Washington, DC: AAG Annual Meeting

Le Néchet F (2012). Urban spatial structure, daily mobility and energy consuption: a study of 34 European cities. Cybergeo

Liu Y, Wang F, Xiao Y, Gao S (2012). Urban land uses and traffic 'source-sink areas': evidence from GPS-enabled taxi data in Shanghai. Landsc Urban Plan, 106(1): 73–87

Long Y, Shen Z (2015). Discovering functional zones using bus smart card data and points of interest in Beijing. In: Long Y, Shen Z, eds. Geospatial Analysis to Support Urban Planning in Beijing. Springer,

193–217

Louw J (2011). Context based detection of urban land use zones. Dissertation for the Doctor Degree. Cape Town: University of Cape Town

Lv Z Q, Dai F Q, Sun C (2012). Evaluation of urban sprawl and urban landscape pattern in a rapidly developing region. Environ Monit Assess, 184(10): 6437–6448

Pan G, Qi G, Wu Z, Zhang D, Li S (2012). Land-use classification using taxi GPS traces. IEEE Trans Intell Transp Syst, 14(1): 113–123

Qi G, Li X, Li S, Pan G, Wang Z, Zhang D (2011). Measuring social functions of city regions from large-scale taxi behaviors. In: 2011 IEEE International Conference on Pervasive Computing and Communications Workshops (PERCOM Workshops). IEEE, 384–388

Simpson W (1992). Urban Structure and the Labour Market: Worker Mobility, Commuting and Underemployment in Cities. Oxford: Clarendon Press, 1–198

Stehman S V (1997). Selecting and interpreting measures of thematic classification accuracy. Remote Sens Environ, 62(1): 77–89

Sohn J (2005). Are commuting patterns a good indicator of urban spatial structure? J Transp Geogr, 13(4): 306–317

Steiniger S, Lange T, Burghardt D, Weibel R (2008). An approach for the classification of urban building structures based on discriminant analysis techniques. Trans GIS, 12(1): 31–59

Vanderhaegen S, Canters F (2017). Mapping urban form and function at city block level using spatial metrics. Landsc Urban Plan, 167: 399–409

Xing H, Meng Y (2018). Integrating landscape metrics and socio-economic features for urban functional region classification. Comput Environ Urban Syst, 72: 134–145

Xing H, Meng Y (2020). Measuring urban landscapes for urban function classification using spatial metrics. Ecol Indic, 108: 105722

Walde I, Hese S, Berger C, Schmullius C (2014). From land cover-graphs to urban structure types. Int J Geogr Inf Sci, 28(3): 584–609

Yang X, Fang Z, Yin L, Li J, Zhou Y, Lu S (2018). Understanding the spatial structure of urban commuting using mobile phone location data: a case study of Shenzhen, China. Sustainability-basel. 10(5):1435

Yoshida T, Tanaka K (2005). Land-use diversity index: a new means of detecting diversity at landscape level. Landscape Ecol Eng, 1(2), 201–206

Zhang J, Goodchild M F (2002). Uncertainty in Geographical Information. London: CRC Press

Zhang C (2008). An analysis of urban spatial structure using comprehensive prominence of irregular areas. Int J Geogr Inf Sci, 22(6): 675–686

Zhang X, Du S, Wang Q (2017). Hierarchical semantic cognition for urban functional zones with VHR satellite images and POI data. ISPRS J Photogramm Remote Sens, 132: 170–184

Zhang C, Sargent I, Pan X, Li H, Gardiner A, Hare J, Atkinson P M (2019a). Joint deep learning for land cover and land use classification. Remote Sens Environ, 221: 173–187

Zhang S, Liu X, Tang J, Cheng S, Wang Y (2019b). Urban spatial structure and travel patterns: analysis of workday and holiday travel using inhomogeneous Poisson point process models. Comput Environ Urban Syst, 73: 68–84

Zhong C, Arisona S M, Huang X, Batty M, Schmitt G (2014). Detecting the dynamics of urban structure through spatial network analysis. Int J Geogr Inf Sci, 28(11): 2178–2199

Zhong C, Huang X, Arisona S M, Schmitt G (2013). Identifying spatial structure of urban functional centers using travel survey data: a case study of Singapore. In: Proceedings of the First ACM SIGSPATIAL International Workshop on Computational Models of Place, Orlando, FL, USA, 2013, 28–33